# Microsolvation of Phenol in Water: Structures, Hydration Free Energy and Enthalpy

Alhadji Malloum[†,◇,*] and Jeanet Conradie[†,‡]

[†] Department of Chemistry, University of the Free State, PO BOX 339, Bloemfontein 9300, South Africa.

[◇] Department of Physics, Faculty of Science, University of Maroua, PO BOX 46, Maroua, Cameroon.

[‡]Department of Chemistry, UiT - The Arctic University of Norway, N-9037 Tromsø, Norway.

December 23, 2022

**ABSTRACT:** In this work, we have studied the microsolvation of phenol in water. We started by identifying initial configurations of phenol-water clusters using classical molecular dynamics. The configurations are optimized at the ωB97XD/aug-cc-pVDZ level of theory. To understand the interaction between phenol and the solvating water molecules, we performed a quantum theory of atoms in molecules (QTAIM) analysis. The results show that the structures of phenol-water clusters are similar to those of neutral water clusters. The QTAIM analysis shows that the structures of phenol-water clusters are stabilized by strong OH···O hydrogen bondings, weak CH···O hydrogen bondings, and OH···π bonding interactions. The located structures of phenol-water clusters have been used to calculate the absolute hydration free energy and enthalpy of phenol for temperatures between 20 and 400 K. The hydration energies are calculated using the cluster continuum solvation model. It has been found that the explicit solvation has negligible effects on the hydration free energy and enthalpy of phenol. Furthermore, the hydration free energy of phenol is found to be linearly varying with increasing temperature, while the hydration enthalpy is found to be temperature independent. The estimated hydration free energy of phenol is slightly underestimated as compared to a previously reported experimental estimate.

**KEYWORDS**: Solvation of phenol; Hydration free energy; Hydrogen bond network; QTAIM analysis; Temperature effects

## 1 Introduction

Phenol is an organic aromatic compound with a hydroxyl OH group soluble in water. It is an important compound used in industry for numerous purposes. Phenol and its derivatives are used, for example, in the synthesis of herbicides (used in agriculture), and several pharmaceutical drugs. Thus, understanding its solvation in water, especially its close interactions with solvent water molecules, is of primary importance. That is the reason why the solvation of phenol in water or the phenol-water cluster has received significant attention in the cluster community. As outlined in the next paragraph, phenol-water clusters have been investigated from several perspectives.

The first perspective was the understanding of the hydrogen bond networks of $PhOH(H_2O)_n$. The study of hydrogen bond networks of the phenol-water clusters, $PhOH(H_2O)_n$, has been reported by several authors [1–11]. Early investigations of the phenol-water clusters have been reported by Watanabe and Iwata [1] at the HF/6-31G(d) level of theory. The authors have reported different configurations of the phenol-water clusters, $PhOH(H_2O)_n$, for $n = 1-5$. Clustering energies, clusters free energies, binding energies, as well as vibration frequencies analysis have been also reported for the studied clusters [1]. In addition, Benoit and Clary [2] reported similar study using an improved computational level of theory, B3LYP/6-311++G(d,p). Guedes *et al.* [3] used three different functionals of DFT (density functional theory) to the study the solvated phenol clusters, for $n = 1-6$. They recommended the B3LYP and B3PW91 hybrid functionals over the BLYP DFT functional, which underestimates the PhO-H bond dissociation energy. Parthasarathi *et al.* [8] reported the investigation of $PhOH(H_2O)_{1-3}$ using *ab-initio* methods and DFT functionals. The authors have also investigated the hydrogen bonding using the quatum theory of atoms in molecules (QTAIM) analysis. Beside *ab-initio* and DFT functionals, molecular dynamics simulations have been also used to study the hydrogen bond networks of the solvated phenol in water [9,11].

The second perspective was the understanding of the vibrational features of the solvated phenol in water. Several authors have reported the electronic, and the infrared or vibrational spectroscopy of $PhOH(H_2O)_n$ for different cluster size [12–18]. Early experimental spectroscopic study of the phenol-water clusters was reported by Fuke and Kaya [12]. The authors reported the $\pi \longrightarrow \pi^*$ electronic absorption of $PhOH(H_2O)_{0-3}$. Janzen *et al.* [14] reported the experimental vibrational spectroscopy of $PhOH(H_2O)_{7,8}$ in the OH stretching region. They found that the vibrational spectra are combination of features from different isomers. Their *ab-initio* calculations showed that the structures of the phenol-water clusters are very similar to those of neutral water clusters [14]. Large sized solvated phenol clusters, $PhOH(H_2O)_n$, $\sim 10 \leq n \leq \sim 50$, have been reported by Mizuse, Hamashima and Fujii [15,16], experimentally. The authors measured the IR spectra of the clusters in the OH-stretching region. The results show that band associated to the free-OH stretching is blue-shifted with the increasing cluster size $n$ [15]. Recently, Katada and Fujii [18] reported the experimental IR spectroscopy of the protonated phenol-water clusters for $n = 1-5$.

The third perspective was the evaluation of the solvation free

* *E-mail: MalloumA@ufs.ac.za; Tel: +237 695 15 10 56*

energy and the solvation enthalpy of phenol in water. Few authors have reported the study of the solvation free energy of phenol in water using different approaches [19–23]. Hydration free energies (i.e. solvation free energies in water) of several molecules have been evaluated by Gallicchio, Zhang and Levy [19] based on surface generalized Born (SGB) continuum dielectric electrostatic model. The model used by the authors is termed as experiment, and the evaluated hydration free energy of phenol is $-6.6\,\mathrm{kcal/mol}$ [19]. Reddy and Erion [20] have reported the relative solvation free energy of phenol⟶benzene using QM/MM (quantum mechanics and molecular mechanics). The relative solvation free energy of phenol⟶benzene is evaluated to be $4.9\,\mathrm{kcal/mol}$. In addition, hydration energies of phenol as well as other molecules have been evaluated using different empirical solvation models by Sharma and Kaminski [21]. The hydration energy of phenol is evaluated to be -6.6, -6.7 and $-5.6\,\mathrm{kcal/mol}$ using Fuzzy-border, Poisson-Boltzmann, and Generalized Born models, respectively [21]. Besides, enthalpies of solvation of phenol and substituted phenols in acetonitrile, tetrahydrofuran, and 1,4-dioxane have been reported by Nagrimanov, Samatov, and Solomonov [22].

Observation of literature reveals that the study of the structures and the hydrogen bond networks of $PhOH(H_2O)_n$ has been limited to small sized clusters. Moreover, even for the small sized clusters, no evidence of global minimum potential energy surfaces (PESs) exploration has been reported. It is worth noting that the accuracy of any study on the solvated phenol clusters depends on the accurate identification of all possible configurations of the clusters. Therefore, it becomes necessary to revisit the study of $PhOH(H_2O)_n$ clusters. Thus, we explored the PESs of the clusters of $PhOH(H_2O)_n$, for $n = 1-12$, using classical molecular dynamics. The obtained configurations are then optimized using a dispersion corrected DFT functional, $\omega$B97XD, associated to the aug-cc-pVDZ basis set. In addition, QTAIM analysis has been performed on the most stable configurations of the phenol-water clusters to identify the interactions between phenol and water molecules. Thermodynamics properties and absolute solvation energies are also provided for temperatures ranging from 20 to 400 K.

## 2 Methodology

### 2.1 Sampling of configurations

To achieve the objectives of this work, we need to identify low lying energy structures of the solvated phenol clusters, $PhOH(H_2O)_n$, $n = 1-12$. Thus, we started by sampling possible structures of different clusters. For each cluster size, initial configurations are generated using the ABCluster code of Zhang and Dolg [24,25]. ABCluster samples all possible configurations and classifies them from the most stable to the least stable configuration based on a classical energy. The classical energy used by ABCluster is constituted of Lennard-Jones potential as well as electrostatic potential. The parameters used are based on CHARMM's force field [26]. Details on how the configurations are generated can be found in our recent works [27–31]. In addition, the reader is advised to read the original papers of Zhang and Dolg [24,25] for more details on ABCluster.

### 2.2 Solvation free energy and enthalpy

In this work, solvation free energy and solvation enthalpy refer to the absolute solvation free energy and the absolute solvation enthalpy of phenol, respectively. The solvation free energy and the solvation enthalpy are calculated in this work using the cluster continuum solvation model (CCM). In the CCM approach the phenol is explicitly solvated with few water molecules, while the remaining solvent is represented by a dielectric continuum medium. The phenol solvation can be represented by Equation 1.

$$\mathrm{Phenol}(g) + (H_2O)_n(s) \longrightarrow \mathrm{Phenol}(H_2O)_n(s) \qquad (1)$$

Then, the absolute solvation free energy and the absolute solvation enthalpy of phenol can be calculated using Equation 2 and Equation 3, respectively.

$$\Delta G_s(\mathrm{Phenol})_n = \Delta G_s[\mathrm{Phenol}(H_2O)_n] - \Delta G_s[(H_2O)_n] - \Delta G_g(\mathrm{Phenol}), \qquad (2)$$

$$\Delta H_s(\mathrm{Phenol})_n = \Delta H_s[\mathrm{Phenol}(H_2O)_n] - \Delta H_s[(H_2O)_n] - \Delta H_g(\mathrm{Phenol}), \qquad (3)$$

where the subscript $s$ stands for the water solvent and the subscript $g$ stands for the gas phase. Thus, the solvation free energy and the solvation enthalpy of phenol in water are obtained when the calculated values of $\Delta G_s(\mathrm{Phenol})_n$ and $\Delta H_s(\mathrm{Phenol})_n$ are not varying with increasing cluster size $n$ (which corresponds to the convergence of the solvation free energies). The CCM approach can be summarized by the the schematic representation of Figure 1.

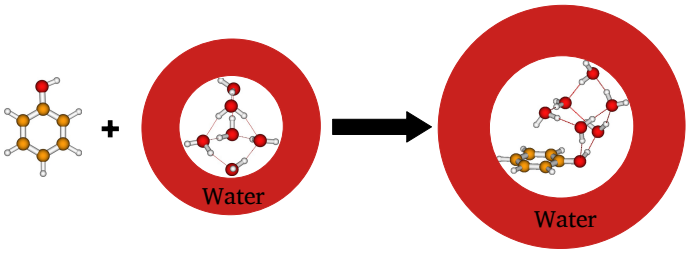


**Fig. 1** Schematic representation of the cluster continuum solvation model (CCM) using six explicit water molecules.

Therefore, it comes out from the above equations and scheme that the calculation of the solvation free energy and enthalpy of phenol depend on the determination of the structures of the solvated phenol clusters, $\mathrm{Phenol}(H_2O)_n$, as well as the structures of neutral water clusters. The structures of the solvated phenol clusters are generated and optimized in this work, while the structures of neutral water clusters are retrieved from our previous works [32,33]. It should be noted that the cluster continuum solvation model has been successfully used in previous works to determine the absolute solvation free energies of the proton and other ions [34–43].

Although not explicitly shown, Equation 2 and Equation 3 are temperature dependent. To calculate the free energy and the enthalpy of Phenol$(H_2O)_n$ and $(H_2O)_n$, we use the free energies of different possible isomers, $G_k(T)$, weighted by their relative probabilities, $W_k(T)$. The relative probabilities are calculated using the Boltzmann distribution:

$$G(T) = \sum_k W_k(T) \times G_k(T), \tag{4}$$

and

$$W_k(T) = \frac{\exp(-\beta G_k(T))}{\sum_i \exp(-\beta G_i(T))}. \tag{5}$$

Thus, the contribution of the isomers to the final free energy of a given cluster is dictated by its Boltzmann weight $W_k(T)$. As will be seen later, most of the isomers do not contribute to the cluster's population or they contribute with negligible probability. It is worth mentioning that the free energies $G_k(T)$ of different isomers as well as the weight $W_k(T)$ are calculated using the Tempo code of Fifen and coworkers[44]. The program Tempo computes the free energies $G_k(T)$ for different values of temperature using the canonical ensemble. To calculate $G_k(T)$, Tempo uses the electronic energies and the harmonic frequencies from the Gaussian output files. With the calculated free energies $G_k(T)$, Tempo computes the weight $W_k(T)$ using the Boltzmann distribution of Equation 5.

### 2.3 Computational details

After sampling all the configurations of the solvated phenol clusters using ABCluster, the generated configurations have been fully optimized at the $\omega$B97XD/aug-cc-pVDZ level of theory. To ensure that we have located the most stable structures, frequencies have been calculated at the same level of theory. It has been checked that no imaginary frequency is found for the reported structures. Besides, the frequencies are also used to calculate the thermodynamics properties (free energies and enthalpies) of the solvated phenol clusters. The optimizations and the calculations of frequencies have been performed using Gaussian 16 suite of program[45]. For accurate optimizations, we used the **tight** option, and **ultrafine** grid for accurate integrals. All optimizations are performed in the implicit solvent phase using the polarizable continuum solvation model[46]. Single point calculations have been performed at the SCS-MP2/aug-cc-pVTZ level of theory. SCS-MP2[47] calculations are performed using Orca computational chemistry program[48]. The single-point calculations are performed in the implicit solvation using the SMD solvation model[49]. The quantum theory of atoms in molecules (QTAIM) analysis has been performed using the AIMAll program[50]. QTAIM analysis has been performed to understand the non-covalent bondings between the water molecules and phenol.

## 3 Results and discussions

As stated in the methodology section, to compute the solvation free energy and enthalpy of phenol we need the structures of the solvated phenol clusters, PhOH$(H_2O)_n$. Thus, we start this section by presenting the located structures of the solvated phenol clusters, PhOH$(H_2O)_n$, $n = 1-12$ (see subsection 3.1). After presenting the structures, we performed a QTAIM analysis on the most stable structures to understand the nature of non-covalent bondings between the solvating water molecules and phenol (see subsection 3.2). The cluster continuum solvation approach presented in the previous section is temperature-dependent. Among the located isomers, only those having non negligible probabilities can contribute to the population of the cluster, and therefore only those isomers can contribute to the calculation of the solvation free energy and enthalpy. Consequently, we presented in subsection 3.3 the probability of all the isomers, for different cluster sizes, as function of temperature. Finally, we reported in subsection 3.4 the calculated absolute solvation free energy and absolute solvation enthalpy of phenol in water. These solvation energies are reported at room temperature as well as at temperatures ranging from 20 to 400 K.

### 3.1 Microsolvation of phenol

The optimized structures of the solvated phenol monomer and dimer are reported in Figure 2.

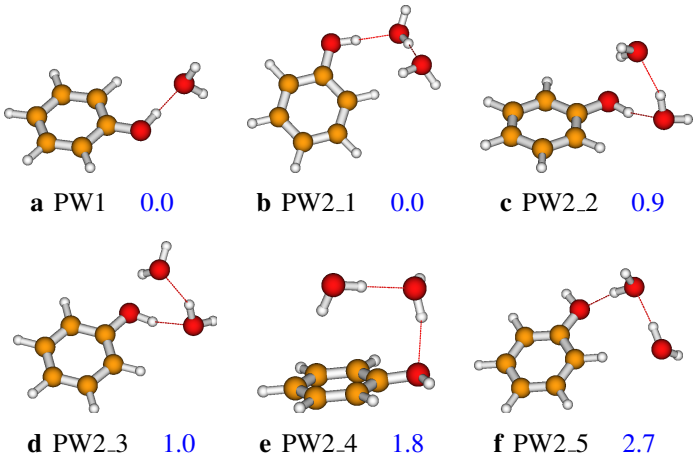


**Fig. 2** Structures of the solvated phenol with one and two explicit water molecules, as optimized at the $\omega$B97XD/aug-cc-pVDZ level of theory.

After generating the initial configurations using ABCluster, optimization have been performed at the $\omega$B97XD/aug-cc-pVDZ level of theory. For the solvated phenol monomer, PhOH$(H_2O)_1$, only one configuration is found to be stable (see **PW1** in Figure 2). In **PW1**, the water molecule establishes one strong OH$\cdots$O hydrogen bond and one weak CH$\cdots$O hydrogen bond with the phenol molecule. In addition, the water molecule acts as a hydrogen bond acceptor, while the OH group of phenol is the hydrogen bond donor (see Figure 2 and Figure 8). For the case of the solvated phenol dimer, PhOH$(H_2O)_2$, eight initial configurations have been optimized; among which, five are found to be different from each other covering an energy cutoff of 2.7 kcal/mol

(see Figure 2). The most stable isomer of the solvated phenol dimer is **PW2_1**. In **PW2_1**, the two water molecules establish one strong OH···O hydrogen bond and two weak CH···O hydrogen bonds with the phenol molecule. In addition, the two water molecules are linked by a strong OH···O hydrogen bond (see Figure 2, and Figure 8). The second and third most stable isomers, **PW2_2** and **PW2_3**, lie 0.9 and 1.0 kcal/mol above the global minimum energy structure. In these two isomers, the two water molecules and the OH group of phenol form a cyclic OH···O hydrogen bondings network (see Figure 2).

It is should be noted that previous works have also reported the **PW1** isomer as the most stable configuration of the phenol-water monomer[1,3,5,8]. Watanabe and Iwata[1] have also reported another stable structure at the HF/6-31G level of theory. That isomer was reported to lie about 3.0 kcal/mol above **PW1**, highlighting its less stability[1]. As far as the phenol-water dimer is concerned, all previous works have reported the cyclic isomers, **PW2_2** and **PW2_3**, to be the most stable isomer. This result is in contradiction with our finding which shows that the isomer **PW2_1** is the most stable. It is worth mentioning that the isomer **PW2_1** is reported here for the first time. There are two possible reasons that can explain the difference in the located most stable configuration of the phenol-water dimer. First, the structures reported in this work are optimized in the solvent phase, while previous works reported gas phase structures. Second, no global optimization has been performed previously, which could have lead to missing isomers (such as **PW2_1**) on the PES of the phenol-water dimer. The isomers **PW2_4** and **PW4_5** are located in this work for the first time.

Fifteen initial geometries of the solvated phenol trimer, $PhOH(H_2O)_3$, have been optimized. After optimization, eleven structures have been located to be different one from another. The retained structures are reported in Figure 3 covering an energy cutoff of 4.2 kcal/mol. The results show that there are three isoenergetically most stable isomers of the solvated phenol trimer, **PW3_1**, **PW3_2**, and **PW3_3** (see Figure 3). For the three isomers, the three water molecules and the phenol OH group form a cyclic OH···O hydrogen bondings network. The difference between the isomers lies in the orientation of the free OH *vis-à-vis* the OH···O plane. This follows the same configurations as the most stable structures of neutral water tetramer[32,51,52]. It has been noted that apart from the three most stable structures, the other isomers establish only one OH···O hydrogen bond with the phenol OH group. We concluded that the stability of the solvated phenol trimers are affected by the number OH···O hydrogen bonds established with phenol. The isomers in which the phenol OH group is both hydrogen bond donor and acceptor is found to be more stable than the isomer in which the phenol OH group establishes only one hydrogen bond, although sometimes with additional OH···$\pi$ or CH···O interactions.

All previous works reported the isomer **PW3_1** to be the most stable configuration of the phenol-water trimer, in agreement with our result[1,3,5,8]. However, two more similar isomers, **PW3_2** and **PW3_3**, have been reported additionally in this work. The three isomers, **PW3_1**, **PW3_2** and **PW3_3** have the same hydrogen bond networks as the most stable isomers of the neutral water tetramer[33]. furthermore, most of the configurations of Figure 3 are located in this work for the first time.

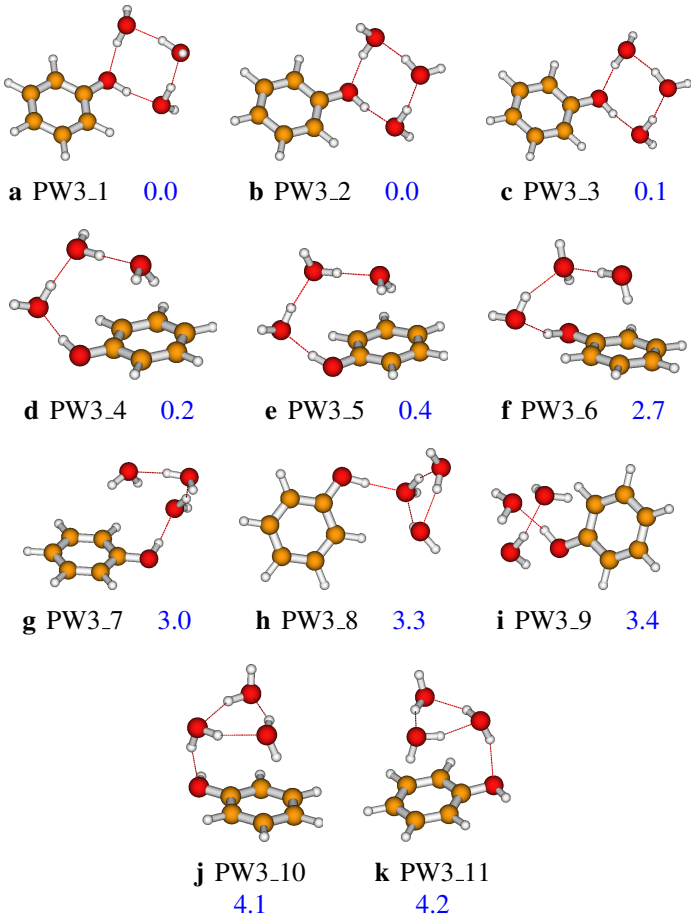


**Fig. 3** Structures of the solvated phenol with three explicit water molecules, as optimized at the $\omega$B97XD/aug-cc-pVDZ level of theory.

Regarding the solvated phenol tetramer, sixteen stable configurations are located on its PES. The located isomers have their relative energies spanning from 0.0 to 2.4 kcal/mol (see Figure 4). The most stable structure, **PW4_1**, has a cyclic OH configuration. In addition to the five strong OH···O hydrogen bondings, **PW4_1** has two weak CH···O hydrogen bondings and one OH···$\pi$ interaction (see Figure 8). The high stability of **PW4_1** is attributed to the fact that it establishes extra bonding interactions in addition to the cyclic OH···O hydrogen bondings. An isomer with cyclic OH configuration has been located by previous authors to be the global minimum structure of the phenol-water tetramer[1,3,5]. In that isomer, the four water molecules as well as the phenol OH group act as proton donor and proton acceptor without further interaction with the phenyl group. After optimization at $\omega$B97XD/aug-cc-pVDZ level of theory, the isomer converged to **PW4_4**. The difference between **PW4_4** and the isomer located in previous works is that in **PW4_4**, the water molecules establish further interactions with the phenyl group through CH···O and OH···$\pi$ interactions. Comparison with pre-

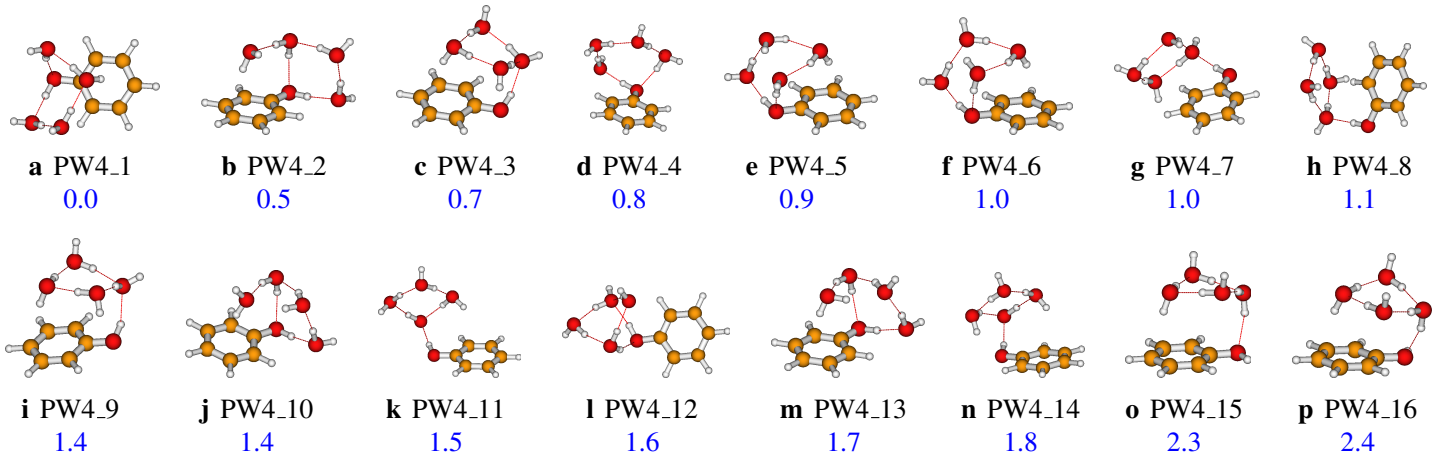


**Fig. 4** Structures of the solvated phenol with four explicit water molecules, as optimized at the ωB97XD/aug-cc-pVDZ level of theory.

vious works shows that all the isomers of Figure 4 are reported in this work for the first time. It is worth mentioning that the location of new isomers in this work has been possible following global optimization using classical molecular dynamics as implemented in ABCluster[24,25]. This essential step in the exploration of the PESs of clusters has been skipped in previous work, which also explains the difference between current work and previous results. As can be seen in Figure 4, the phenol OH group of low lying energy structures (from **PW4_1** to **PW4_6**) acts as proton donor and proton acceptor, establishing therefore two strong hydrogen bonds with the solvating water molecules. However, in less stable structures, the phenol OH group is either a proton donor or proton acceptor, establishing only one hydration bond (see **PW4_14**, **PW4_15** and **PW4_16** in Figure 4).

Initially, twenty geometries of the phenol-water hexamer have been optimized at the ωB97XD/aug-cc-pVDZ level of theory. After optimization, sixteen structures are found to be stable and different one from another. The located structures, covering an energy cutoff of 2.5 kcal/mol, are reported in Figure 5. The most stable structure, **PW6_1**, exhibits a cage like configuration similar to the case of water heptamer. In addition to strong OH···O hydrogen bondings, **PW6_1** has further bonding interactions resulting from the interaction of the water molecules with the phenyl group (see Figure 8). Exploration of the literature shows that few authors investigated the hydrogen bond networks of phenol-water clusters larger than the pentamer. Guedes *et al.*[3] reported an isomer with double cyclic OH configuration as the most stable structure of the phenol-water hexamer. It should be noted that in the configuration located by Guedes *et al.*[3], the water molecules do not interact with the phenyl group. This is due to the lack of correlation (dispersion interactions) in the HF method used by the authors. On the other hand, after taking into account the dispersion corrections in this work (through the ωB97XD DFT functional), all the located isomers interact with the phenyl group in addition to the OH···O hydrogen bondings (see Figure 5). In addition, examination of the structures shows that the hydrogen bond network of the phenol-water hexamer is similar to that of neutral water heptamer. However, the phenol-water hexamer structures

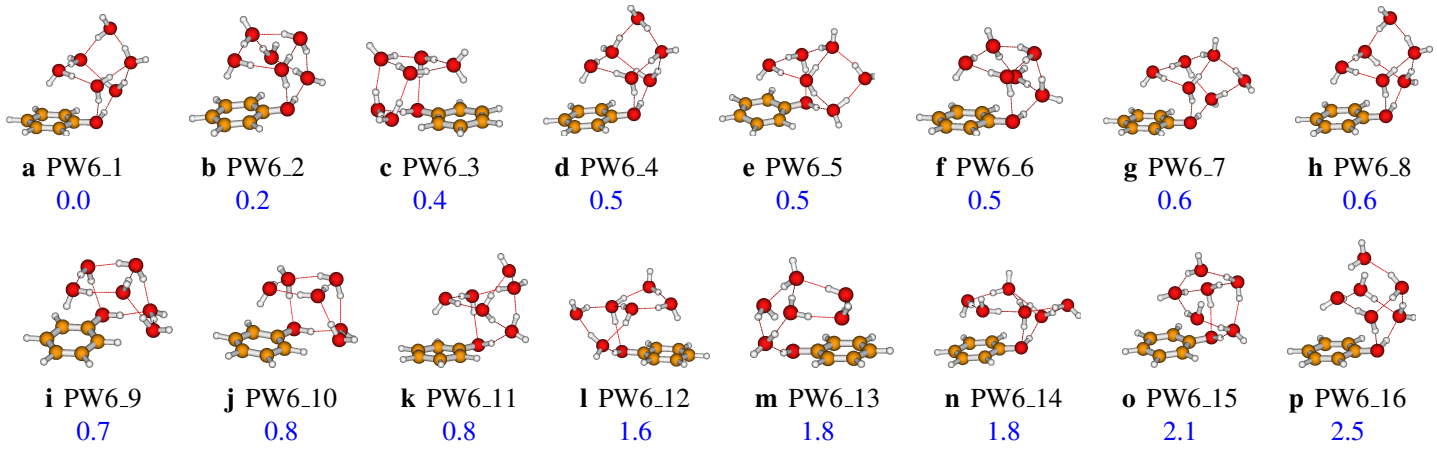


**Fig. 5** Structures of the solvated phenol with six explicit water molecules, as optimized at the ωB97XD/aug-cc-pVDZ level of theory.

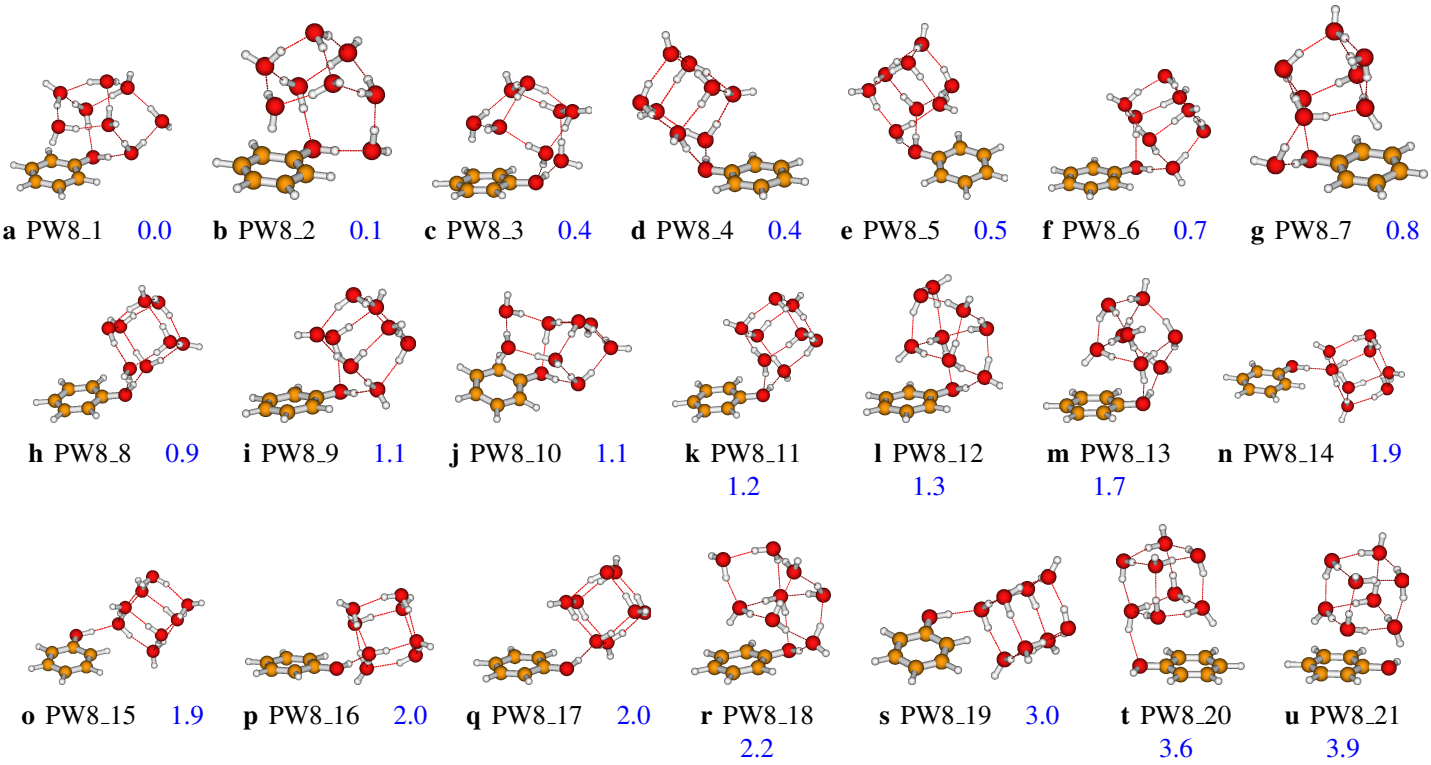


**Fig. 6** Structures of the solvated phenol with eight explicit water molecules, as optimized at the ωB97XD/aug-cc-pVDZ level of theory.

establish further interactions with phenyl group, generating lesser free OH stretching.

The number of possible isomers on the PESs of the phenol-water clusters increases with the cluster size. For the phenol-water octamer, among the twenty five optimized configurations, twenty one are retained and reported in Figure 6. The isomers are located within the cutoff energy of 3.9 kcal/mol. The most stable configuration of the octamer, **PW8_1**, has a folded cage structure. The folding originates from the interaction of one water molecule with the phenyl group. Thus, in addition to the OH···O hydrogen bondings, **PW8_1** has one CH···O and one OH···$\pi$ bonding interactions (see Figure 8). As can be seen in Figure 6, almost all the isomers have cage like structures, where most of them are folded cage. Previously, Janzen *et al.*[14] investigated the experimental spectroscopy of $PhOH(H_2O)_{7,8}$, and reported some *ab-initio* calculations. Their located stable configurations are similar to **PW8_4** and **PW8_5**, lying 0.4 and 0.5 kcal/mol in this work, respectively (see Figure 6). Similarly, Roth *et al.*[13] located isomers similar to **PW8_5** and **PW8_14**, for their spectroscopic study of the solvated phenol in water. Apart from these three isomers that have been reported previously, the remaining isomers of Figure 6 are located in this work for the first time. Examination of the configurations shows that the configurations of phenol-water octamer are similar to the structures of neutral water nonamer, where the OH of phenol is considered to be the ninth water molecule[33]. In addition, we noted that the hydrogen bond network governs the stability of the isomers. In the low lying energy structures, the phenol OH group establishes two strong hydrogen bondings with the surrounding water molecules. However, for the less stable structures, the phenol OH group is only involved in one hydrogen bonding (see Figure 6). Moreover, low lying energy structures have strong interaction with the phenyl group through CH···O and OH···$\pi$ interactions (see Figure 8).

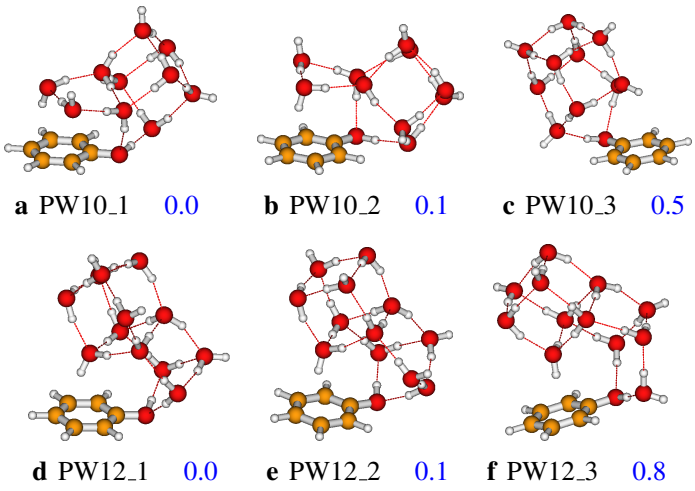


**Fig. 7** The three most stable structures of the solvated phenol with ten and twelve explicit water molecules, as optimized at the ωB97XD/aug-cc-pVDZ level of theory.

Regarding the structures of the solvated phenol decamer and dodecamer, $PhOH(H_2O)_{10}$ and $PhOH(H_2O)_{12}$, we have reported

in Figure 7 only the three most stable structures to avoid cumbersome results. For the decamer, 20 isomers have been located within a relative energy cutoff of 3.6 kcal/mol, while for the dodecamer, 25 different isomers have been located on its PES within a relative energy cutoff of 4.9 kcal/mol. The complete list of the located isomers of the decamer and the dodecamer are presented in the supporting information. Similar to the case of lower size clusters, it is noted that the most stable configurations of the decamer and dodecamer are the isomers where the water molecules establish at least two strong hydrogen bonds and one CH$\cdots\pi$ bonding interaction with the phenyl group (see Figure 7 and Figure 8). For both decamer and dodecamer, the low lying energy level on their PESs is degenerated. The difference between the two isomers lie in the spatial orientation the solvating water molecules. The results show that in the less stable structures, the solvating water molecules establish only one hydrogen bond with phenol. Overall, it is noted that the higher the interaction of the water molecules with phenol, the higher the stability of the corresponding isomer, no matter the internal configuration of the solvating water molecules.

### 3.2 QTAIM analysis of non covalent bondings

To provide more insights about the interaction between the phenol and the solvating water molecules, we performed a QTAIM analysis on the most stable structures of the studied clusters. The located critical points and bond paths of the low lying energy isomers are reported in Figure 8. For the specific case of the phenol-water monomer, we have additionally reported the electron density ($\rho$) two-dimensional contour and the atomic basins in the phenyl plane (see Figure 9). The bond paths, the critical points, the electron density 2D contour, and the the atomic basins of **PW1** indicate the presence of two non-covalent intermolecular bondings, OH$\cdots$O and CH$\cdots$O hydrogen bondings. Quantitative data at all bond critical points (BCPs) are provided in the supporting information. The positive values of the Laplacian of the electron density, $\nabla^2\rho$ (0.1329 au and 0.0260 au), at the bond critical points (of OH$\cdots$O and CH$\cdots$O hydrogen bondings, respectively) are indicative of non-covalent interactions. In addition, for the two BCPs, the electron density is evaluated to be 0.0364 au and 0.0071 au, respectively. These values indicate that the OH$\cdots$O hydrogen bonding is considerably stronger than the CH$\cdots$O hydrogen bonding in **PW1**. We have reported in Table 1 the interval of $\rho$ and $\nabla^2\rho$ at bond critical points of the most stable configurations of the phenol-water clusters.

It can be seen in Figure 8 that the number of non-covalent interactions in phenol-water clusters is dominated by OH$\cdots$O hydrogen bondings. The OH$\cdots$O hydrogen bondings are also found to be the strongest non-covalent interactions of PhOH$(H_2O)_n$ based on the values of the electron density at BCPs (see Table 1). Besides, it is also reflected in Table 1 that the CH$\cdots$O hydrogen bondings are less stronger than the OH$\cdots$O hydrogen bondings in all the studied cluster. In addition to the OH$\cdots$O and the CH$\cdots$O hydrogen bondings, two other non-covalent interactions can be identified in phenol-water clusters: the OH$\cdots\pi$ and the O$\cdots$C bonding interactions (see Figure 8 and Table 1). Among all the non-covalent bondings, the O$\cdots$C bonding interactions are the weakest interactions in phenol-water clusters. We have noted that only few of the OH$\cdots\pi$ and the O$\cdots$C bonding inter-

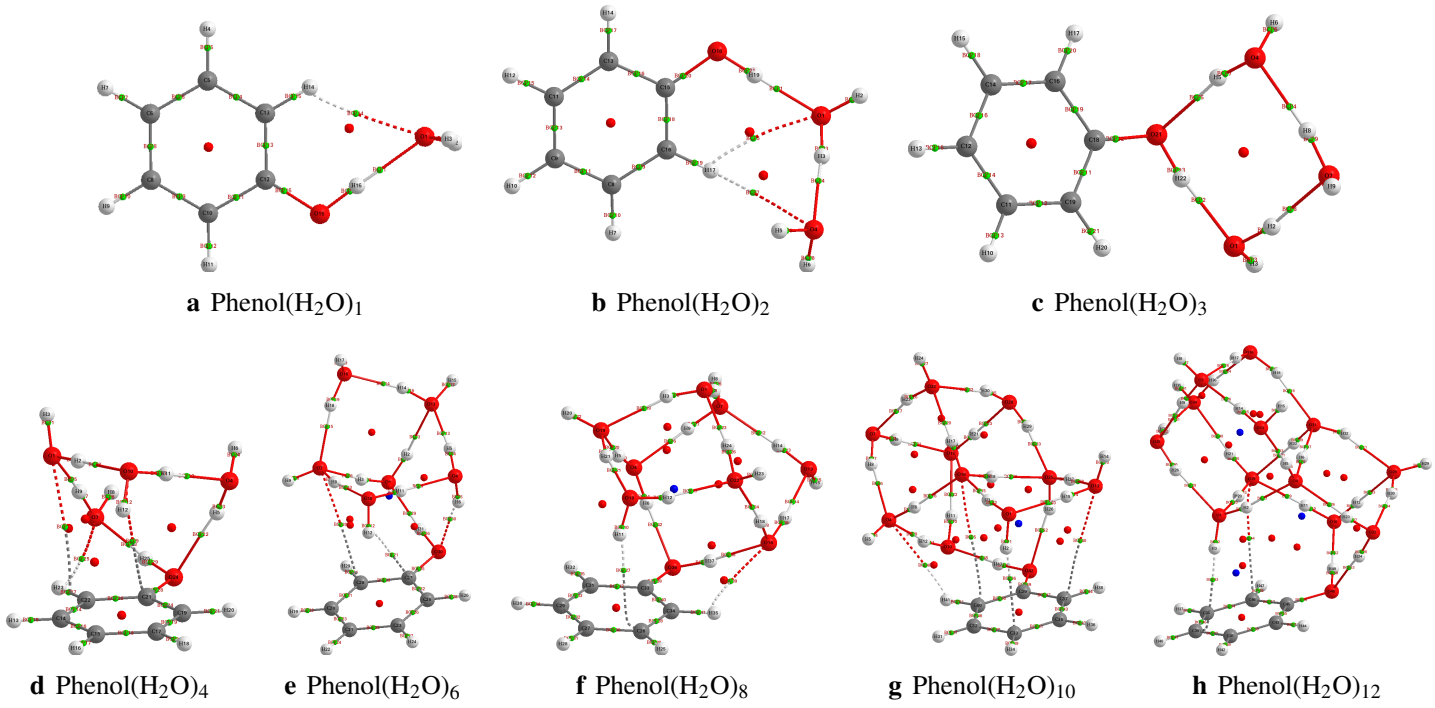

**a** Phenol$(H_2O)_1$ **b** Phenol$(H_2O)_2$ **c** Phenol$(H_2O)_3$

**d** Phenol$(H_2O)_4$ **e** Phenol$(H_2O)_6$ **f** Phenol$(H_2O)_8$ **g** Phenol$(H_2O)_{10}$ **h** Phenol$(H_2O)_{12}$

**Fig. 8** QTAIM analysis of the solvated phenol clusters, PhOH$(H_2O)_n$, $n = 1-12$, using the most stable structures: bond paths and critical points.

actions are identified in this work. Parthasarathi, Subramanian, and Sathyamurthy[8] have reported the QTAIM study of phenol-water monomer, dimer and trimer based on HF/6-31G electron density. The authors found that only the phenol-water monomer and phenol-water trimer have each one CH···O hydrogen bonding. For all the studied clusters, they have only reported OH···O hydrogen bondings[8]. This could be attributed to the quality of their electron density which is calculated at a relatively poor computational level of theory. In addition, their results could also be attributed to the missing isomers of the phenol-water clusters which are located in this work for the first time.

**Table 1** Interval of $\rho$ and $\nabla^2\rho$ at bond critical points of the most stable configurations of the phenol-water clusters, $n = 1-12$, at the $\omega$B97XD/aug-cc-pVDZ level of theory.

| | $\rho$ ($ea_0^{-3}$) | | $\nabla^2\rho$ ($ea_0^{-5}$) | |
|---|---|---|---|---|
| Bonding | Min | Max | Min | Max |
| OH···O | 0.0245 | 0.0512 | 0.0783 | 0.1613 |
| CH···O | 0.0066 | 0.0079 | 0.0211 | 0.0300 |
| OH···$\pi$ | 0.0071 | 0.0112 | 0.0228 | 0.0296 |
| O···C | 0.0027 | 0.0067 | 0.0087 | 0.0226 |

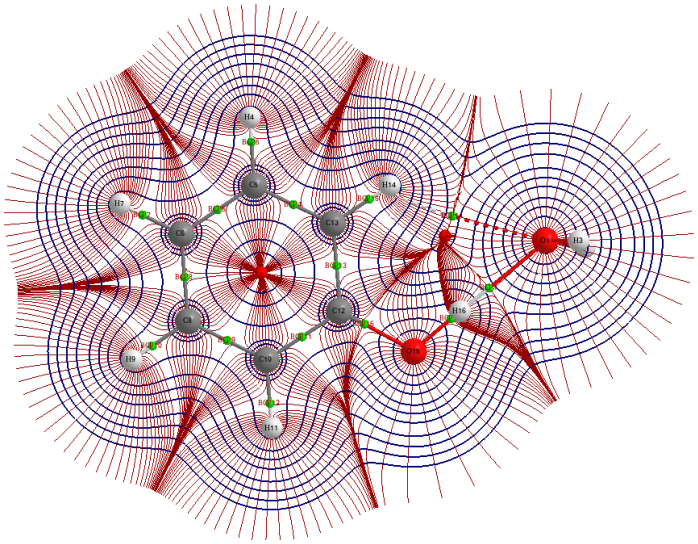

**Fig. 9** QTAIM analysis of $PhOH(H_2O)_1$ using **PW1**: bond paths, critical points, 2-dimensional electron density contour, and atomic basins.

### 3.3 Temperature-dependent isomers' probabilities

Temperature effects on the stability of the investigated clusters is assessed using the Boltzmann distribution. The probabilities (relative populations) of different isomers of the phenol-water clusters are calculated for temperatures ranging from 20 to 400 K. As only one isomer of the monomer is located, there is no need to determine the probability. The calculated probabilities of the phenol-water dimer are plotted as function of temperature in Figure 10. The relative population or probability is the Boltzmann distribution given in Equation 5. The results show that the most stable phenol-water dimer, **PW2_1**, is the most favoured isomer for all the investigated temperatures. The isomers **PW2_2** and **PW2_3** contribute in trace to the population of the phenol-water dimer at high temperatures. The population of the dimer shows that the isomers **PW2_4** and **PW2_5** have negligible contribution to the cluster's population. As noted in our previous works, the isomers with relative energies higher than $\sim$1.0 kcal/mol have negligible contribution to the cluster's population.

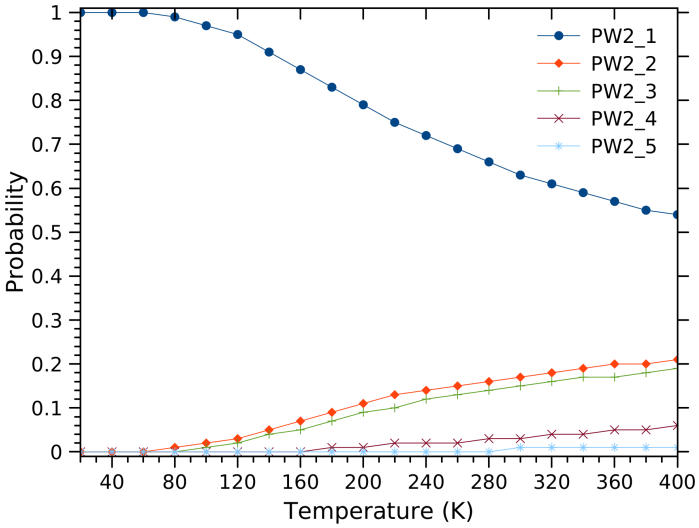


**Fig. 10** Relative population of the solvated phenol with two explicit water molecules, $PhOH(H_2O)_2$. The relative population is the Boltzmann distribution given in Equation 5.

In addition to the phenol-water dimer, we have plotted in Figure 11 the temperature-dependence probabilities of the isomers of the studied clusters. For all the studied clusters, the results show that the most stable configuration is the most favoured at all temperatures. Nevertheless, at high temperatures, other isomers contribute significantly to the population of the clusters. For most of the clusters, there is a competition between the isomers at high temperatures. This result is found be to in agreement with previous works on furan clusters and dimethylsulfoxide clusters[53,54]. We have learnt from the study of the temperature effects that the isomers that significantly contribute to the population of the clusters have their relative energies within $\sim$1.0 kcal/mol. This has been also remarked in our previous work on dimethylformamide clusters[55]. Although the structures of phenol-water clusters have similar configurations to those of neutral water clusters, their temperature-dependence follows different trends. It has been found that several isomers compete to the population of neutral water clusters, with some favoured at low temperatures and others more favoured at high temperatures[51,52,56–58]. However, for the case of the phenol-water cluster, the most stable configurations dominate the population of the clusters. This indicates that the phenyl group has significant influence on the temperature-dependence trend.

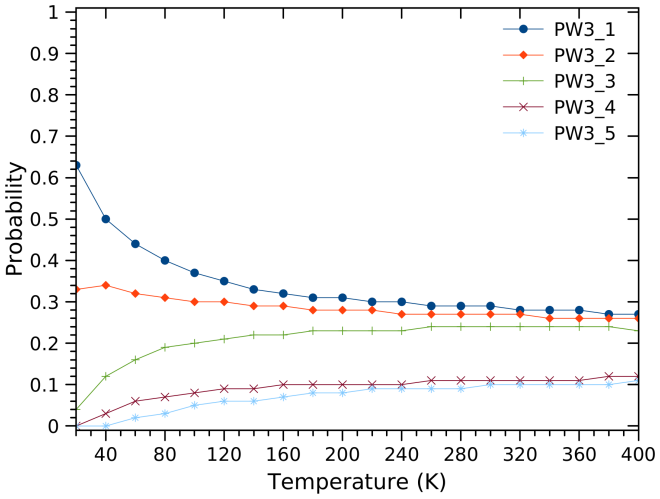


**a** Probability of Phenol$(H_2O)_3$

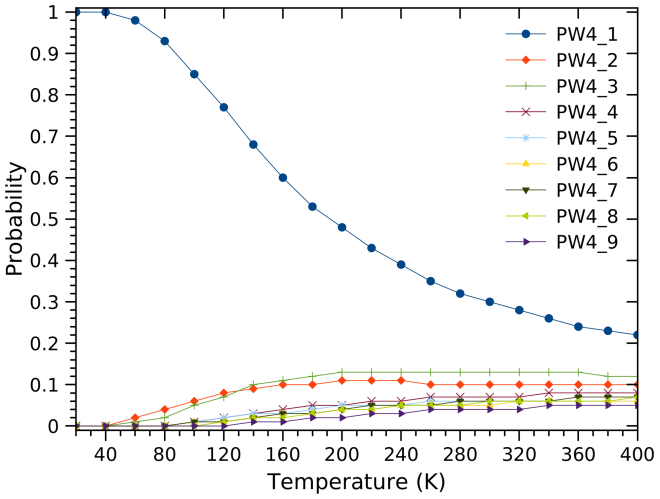


**b** Probability of Phenol$(H_2O)_4$

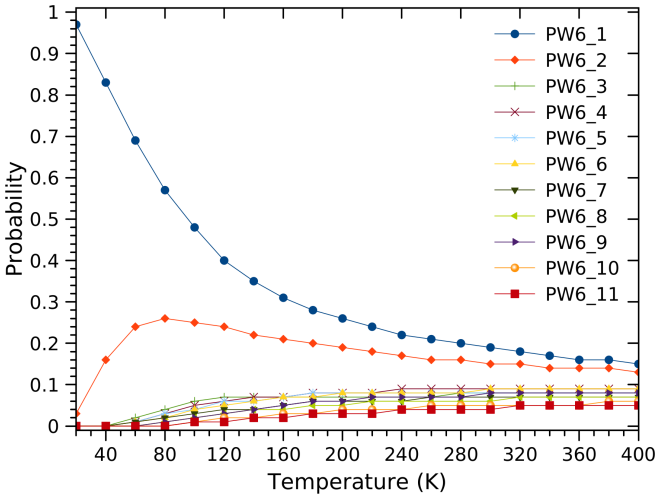


**c** Probability of Phenol$(H_2O)_6$

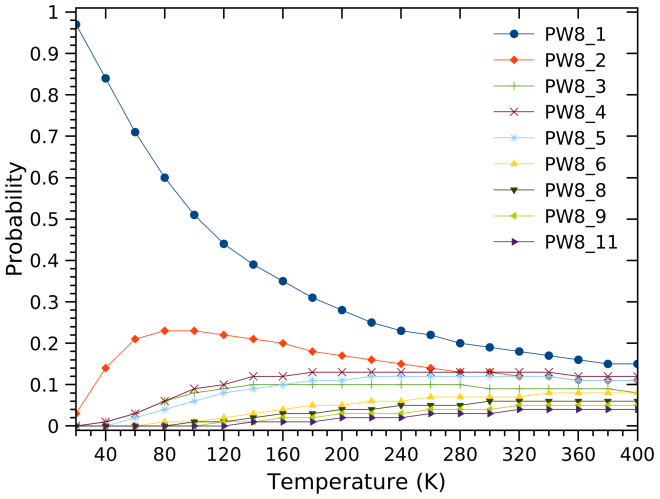


**d** Probability of Phenol$(H_2O)_8$

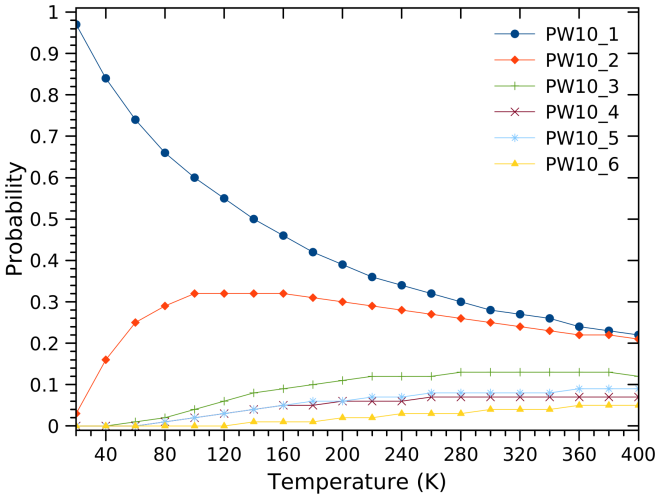


**e** Probability of Phenol$(H_2O)_{10}$

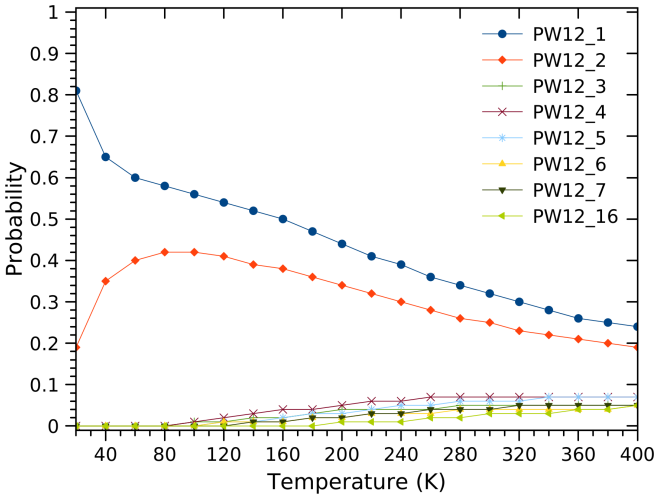


**f** Probability of Phenol$(H_2O)_{12}$

**Fig. 11** Relative population of the solvated phenol clusters in water, $PhOH(H_2O)_n$, $n = 3 - 12$, as computed at the $\omega$B97XD/aug-cc-pVDZ level of theory. The relative population is the Boltzmann distribution given in Equation 5.

### 3.4 Hydration free energies and enthalpies of phenol

Before presenting the calculated hydration free energies and enthalpies of phenol, we would like to properly situate the reader about these properties/energies. The hydration free energies are important to understand chemical reactivity and chemical kinetics of molecules in solvents. They are also involved in several chemical and biological processes as outlined in our previous work[42]. In this work, we use the cluster continuum² solvation model (CCM) to compute the absolute hydration free energy and enthalpy of phenol. As pointed out in the methodology, the CCM has been widely used to calculate the absolute hydration free energy with high accuracy as compared to experiment[34,38,39]. In cluster continuum model, a few explicit solvent molecules around the solute are treated quantum mechanically, while the remaining is considered as a continuum medium. This model is quantum mechanically representing the solvation of a solute in a liquid.

Using the cluster continuum solvation model as outlined in the methodology section, we have calculated the absolute solvation free energy and the absolute solvation enthalpy of phenol in water. The solvation free energy and enthalpy are calculated using Equation 2 and Equation 3, respectively. For each cluster size, we used all the possible configurations as presented in subsection 3.1 weighted by their canonical probabilities. The structures of neutral water clusters are retrieved from our previous works and re-optimized at the ωB97XD/aug-cc-pVDZ level of theory. For the neutral water clusters, only the most stable configurations have been used. To be used in Equation 2 and Equation 3 the gas phase geometry of phenol has been optimized at the ωB97XD/aug-cc-pVDZ level of theory. The solvation free energy and enthalpy of phenol in water are calculated for temperatures ranging from 20 to 400 K. We reported in Figure 12 the variation of the solvation free energy and enthalpy of phenol in water as function of the cluster size $n$ at room temperature (298.15 K).

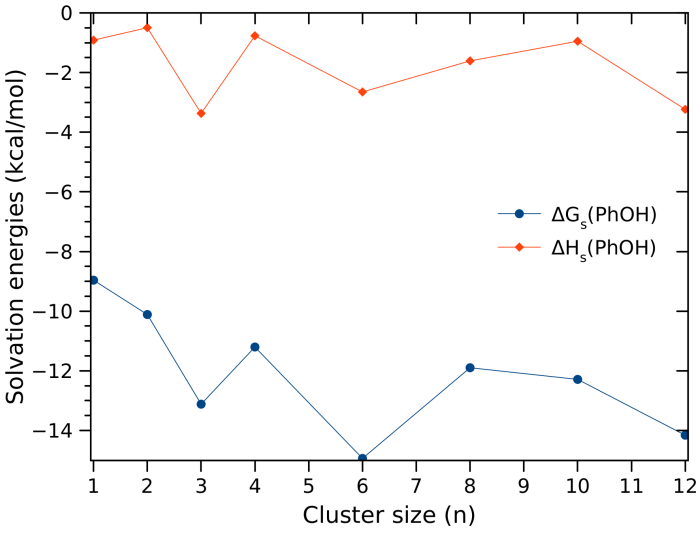


**Fig. 12** Variation of the solvation free energy and enthalpy with the cluster size $n$ for room temperature (298.15 K).

As can be seen in Figure 12, the calculated solvation free energies and enthalpies for different cluster sizes can be regarded as values oscillating around an average. The fact that the values oscillate around an average indicates that the explicit solvation of phenol has a negligible effect on the calculated hydration free energy and enthalpy. The estimated average values of the hydration free energy and enthalpy of phenol are −1.7 kcal/mol and −12.1 kcal/mol, respectively. Previously, an estimate of −6.6 kcal/mol has been reported by Gallicchio, Zhang and Levy[19] for the hydration free energy of phenol. The same value has been reported earlier by Cabani and coworkers[59]. As compared to theirs, our estimated hydration free energy is underestimated (less negative). Our most negative estimate of the hydration free energy (−3.4 kcal/mol found for $n = 3$) is also slightly underestimated as compared to the value estimated by Gallicchio, Zhang and Levy[19]. When no explicit water molecule is used, the hydration free energy of phenol is evaluated to be −4.3 kcal/mol. It is worth noting that the method used by Gallicchio, Zhang and Levy[19] is among the experimental techniques used to estimate the hydration free energy. Therefore, our calculated hydration free energy is slightly underestimated.

Regarding the hydration enthalpy of phenol, a previous experimental estimate of −13.6 kcal/mol has been reported by Cabani and coworkers[59]. Although our estimated hydration free energy is found to be slightly underestimated, our estimated hydration enthalpy is in good agreement with experiment. However, an improvement of the estimates would be interesting. To improve the agreement between our estimates and the experiment, one could use a high level *ab-initio* method which could be expensive for such a large system. Another way is to benchmark several DFT functionals and select the one providing better agreement with the experiment. In addition, Guedes *et al.*[60] have estimated several values of the hydration enthalpy of phenol depending on the potential model used in their Monte Carlo simulations. Their estimations vary from −14.9 kcal/mol to −17.8 kcal/mol[60].

To get further insights into the accuracy of the level of theory and the implicit solvation model, we tried a different level of theory and a different solvation model. Thus, we performed a single-point calculations on the most stable configurations for each value of $n$. The single-point calculations are performed using the SCS-MP2/aug-cc-pVTZ level of theory, and the SMD solvation model. The free energies and enthalpies at the SCS-MP2/aug-cc-pVTZ are obtained using the frequencies calculated at the ωB97XD/aug-cc-pVDZ level of theory. The calculated solvation free energy and enthalpy, for each cluster size $n$, are reported in the supporting information (Table S1). Similar to the case of ωB97XD/aug-cc-pVDZ, the results at the SCS-MP2/aug-cc-pVTZ level of theory show that the solvation free energy and enthalpy oscillate around an average. The averaged values of the solvation free energy and enthalpy are evaluated to be −0.8 kcal/mol and −11.3 kcal/mol, respectively. It comes out from this investigation that the difference between the predictions at these two levels of theory is less than 0.9 kcal/mol.

After examining the effects of explicit solvation, we have investigated the effects of temperature on the hydration free energy and enthalpy for temperatures between 20 and 400 K. The esti-

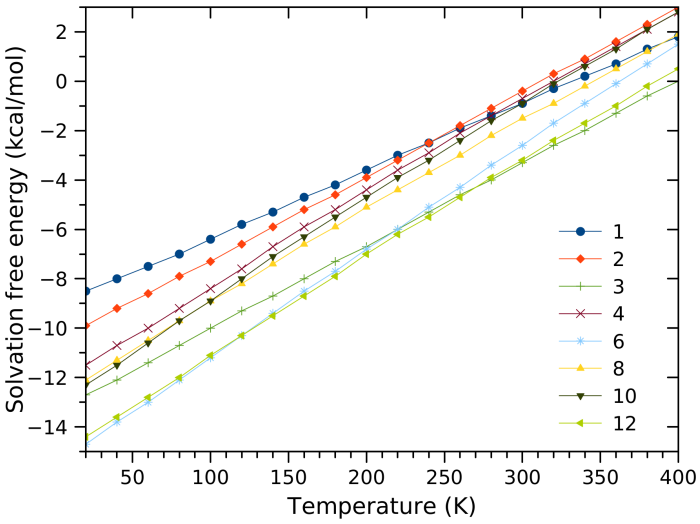


**Fig. 13** Variation of the solvation free energy of phenol in water as function of temperature for different number of explicit solvent molecules, $n = 1 - 12$.

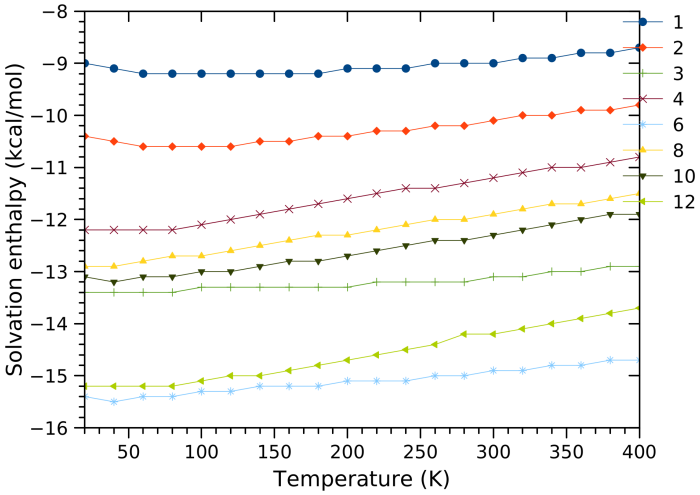


**Fig. 14** Variation of the solvation enthalpy of phenol in water as function of temperature for different number of explicit solvent molecules, $n = 1 - 12$.

mated hydration free energy and enthalpy of phenol as function of temperature for $n = 1 - 12$ are reported in Figure 13 and Figure 14, respectively. The oscillation of the estimated hydration free energy and enthalpy can be seen in Figure 13 and Figure 14. The results show that the hydration enthalpy for a given cluster size is slowly varying with the change of temperature. This could indicate that the hydration enthalpy is temperature independent. Elsewhere, the hydration free energy is varying almost linearly as function of temperature (see Figure 13). This indicates that the variation of the hydration free energy of phenol depends on the slope of the curves (which is the hydration entropy). Thus, one can state that the variation of the hydration free energy of phenol is entropically driven. It is worth noting that this behaviour of the hydration free energy and enthalpy of the proton has been reported in our previous works[40,61]. We have found that the solvation free energy of the proton in ammonia varies linearly as function of temperature, while the solvation enthalpy of the proton in ammonia is found to be temperature independent[40]. Recently, we calculated the adsorption free energy of aniline onto coronene as function of temperature[61]. It has been found that the adsorption free energy is linearly varying with temperature, and entropically driven[61].

## 4 Conclusions

In this work, we provided the absolute hydration free energy and the absolute hydration enthalpy of phenol in water for temperatures ranging from 20 to 400 K. To undertake this investigation, we generated initial configurations of phenol-water clusters for $n = 1$ to $n = 12$. The generated configurations have been optimized at the $\omega$B97XD/aug-cc-pVDZ level of theory. The results show that the configurations of the phenol-water clusters are similar to those of neutral water clusters without the phenol added. However, the configurations phenol-water clusters are folded as compared to neutral water clusters, due to the interaction of water molecules with the phenyl group. To understand the nature of the interaction between the water molecules and phenol, we performed a QTAIM analysis on the most stable structures of the phenol-water clusters. The analysis shows that the structures are stabilized by strong OH$\cdots$O hydrogen bondings and weak CH$\cdots$O hydrogen bondings. In addition, OH$\cdots\pi$ and O$\cdots$C bonding interactions are also identified.

The located structures of phenol-water clusters are used to compute the solvation free energy and enthalpy. Before that, we examined their relative population (probabilities) for temperatures ranging from 20 to 400 K. The results show that the most stable configurations dominate the population of the clusters. In addition, we have found that few structures compete to the population of clusters at high temperatures. After calculating the hydration free energy and enthalpy of phenol, the results show that the explicit solvation has negligible effect on the estimated values. The estimated average values of the hydration free energy and enthalpy of phenol are $-1.7$ kcal/mol and $-12.1$ kcal/mol, respectively. The temperature-dependence of the solvation free energy and enthalpy shows that the hydration enthalpy of phenol is temperature independent, while the hydration free energy varies linearly as function of temperature.

## Acknowledgements

The authors are grateful to the Center for High Performance Computing (CHPC) in South Africa for granting them access to their clusters and computational resources. The Norwegian Supercomputing Program (UNINETT Sigma2, Grant No. NN9684K) is acknowledged for computer time. We would also like to thank the Central Research Fund of the University of the Free State.

## Disclosure statement

There are no conflicts of interest to declare.

## Data availability statement

The data used in this work is provided in the manuscript or in the supporting information.

## Supporting information

Complete list of the optimized structures of the phenol-water decamer and dodecamer, as well as their relative electronic energies are provided. In addition, Cartesian coordinates of the optimized geometries of the clusters are provided. QTAIM analysis data are also reported.

## References


1 Watanabe, H.; Iwata, S. Theoretical studies of geometric structures of phenol-water clusters and their infrared absorption spectra in the O–H stretching region. *J. Chem. Phys.* **1996**, *105*, 420–431.

2 Benoit, D. M.; Clary, D. C. Quantum simulation of phenol- water clusters. *J. Phys. Chem. A* **2000**, *104*, 5590–5599.

3 Guedes, R.; Costa Cabral, B.; Martinho Simoes, J.; Diogo, H. Thermochemical Properties and Structure of Phenol-$(H_2O)_{1-6}$ and Phenoxy-$(H_2O)_{1-4}$ by Density Functional Theory. *J. Phys. Chem. A* **2000**, *104*, 6062–6068.

4 Cabral do Couto, P.; Guedes, R.; Costa Cabral, B.; Martinho Simoes, J. Phenol O–H bond dissociation energy in water clusters. *Int. J. Quantum Chem.* **2002**, *86*, 297–304.

5 Ahn, D.-S.; Jeon, I.-S.; Jang, S.-H.; Park, S.-W.; Lee, S.-Y.; Cheong, W.-J. Hydrogen bonding in aromatic alcohol-water clusters: A brief review. *Bull. Korean Chem. Soc.* **2003**, *24*, 695–702.

6 Ahn, D.-S.; Lee, S.-Y.; Cheong, W.-J. Computational study of hydrogen bonding in phenol-acetonitrile-water clusters. *Bull Korean Chem Soc* **2004**, *25*, 1161–1164.

7 Coutinho, K.; Cabral, B. C.; Canuto, S. Can larger dipoles solvate less? solute–solvent hydrogen bond and the differential solvation of phenol and phenoxy. *Chem. Phys. Lett.* **2004**, *399*, 534–538.

8 Parthasarathi, R.; Subramanian, V.; Sathyamurthy, N. Hydrogen bonding in phenol, water, and phenol- water clusters. *J. Phys. Chem. A* **2005**, *109*, 843–850.

9 Estácio, S. G.; Cabral, B. C. Born–Oppenheimer molecular dynamics of phenol in a water cluster. *Chem. Phys. Lett.* **2008**, *456*, 170–175.

10 José, C. V.; Sandra, C. O.; Fernando, C. G.; Pedro, C. P.; Liadys, M. L. Computational Study of Hydrogen Bonding in Substituted Phenol-Acetonitrile-Water Clusters. *J. Chin. Chem. Soc.* **2008**, *55*, 529–534.

11 Cota, R.; Tiwari, A.; Ensing, B.; Bakker, H. J.; Woutersen, S. Hydration interactions beyond the first solvation shell in aqueous phenolate solution. *Phys. Chem. Chem. Phys.* **2020**, *22*, 19940–19947.

12 Fuke, K.; Kaya, K. Electronic absorption spectra of phenol-$(H_2O)_n$ and $(phenol)_n$ as studied by the MS MPI method. *Chem. Phys. Lett.* **1983**, *94*, 97–101.

13 Roth, W.; Schmitt, M.; Jacoby, C.; Spangenberg, D.; Janzen, C.; Kleinermanns, K. Double resonance spectroscopy of phenol$(H_2O)_{1-12}$: Evidence for ice-like structures in aromate–water clusters? *Chem. Phys.* **1998**, *239*, 1–9.

14 Janzen, C.; Spangenberg, D.; Roth, W.; Kleinermanns, K. Structure and vibrations of phenol$(H_2O)_{7,8}$ studied by infrared-ultraviolet and ultraviolet-ultraviolet double-resonance spectroscopy and ab initio theory. *J. Chem. Phys.* **1999**, *110*, 9898–9907.

15 Mizuse, K.; Hamashima, T.; Fujii, A. Infrared spectroscopy of phenol-$(H_2O)_{n>10}$: structural strains in hydrogen bond networks of neutral water clusters. *J. Phys. Chem. A* **2009**, *113*, 12134–12141.

16 Hamashima, T.; Mizuse, K.; Fujii, A. Spectral signatures of four-coordinated sites in water clusters: Infrared spectroscopy of phenol-$(H_2O)_n$ ($\sim 20 \leq n \leq \sim 50$). *J. Phys. Chem. A* **2011**, *115*, 620–625.

17 Shimamori, T.; Fujii, A. Infrared spectroscopy of warm and neutral phenol–water clusters. *J. Phys. Chem. A* **2015**, *119*, 1315–1322.

18 Katada, M.; Fujii, A. Infrared spectroscopy of protonated phenol–water clusters. *J. Phys. Chem. A* **2018**, *122*, 5822–5831.

19 Gallicchio, E.; Zhang, L. Y.; Levy, R. M. The SGB/NP hydration free energy model based on the surface generalized born solvent reaction field and novel nonpolar hydration free energy estimators. *J. Comput. Chem.* **2002**, *23*, 517–529.

20 Reddy, M. R.; Erion, M. D. Relative solvation free energies calculated using an ab initio QM/MM-based free energy perturbation method: dependence of results on simulation length. *J. Comput. Aided Mol. Des.* **2009**, *23*, 837–843.

21 Sharma, I.; Kaminski, G. A. Calculating pKa values for substituted phenols and hydration energies for other compounds with the first-order fuzzy-border continuum solvation model. *J. Comput. Chem.* **2012**, *33*, 2388–2399.

22 Nagrimanov, R. N.; Samatov, A. A.; Solomonov, B. N. Non-additivity in the solvation enthalpies of substituted phenols and estimation of their enthalpies of vaporization/sublimation at 298.15 K. *J. Mol. Liq.* **2016**, *221*, 914–918.

23 Nagrimanov, R. N.; Ibragimova, A. R.; Solomonov, B. N. Enthalpies of sublimation and vaporization of poly-substituted phenols containing intramolecular hydrogen bonds by solution calorimetry method. *Thermochim. Acta* **2020**, *692*, 178733.

24 Zhang, J.; Dolg, M. ABCluster: the artificial bee colony algorithm for cluster global optimization. *Phys. Chem. Chem. Phys.* **2015**, *17*, 24173–24181.

25 Zhang, J.; Dolg, M. Global optimization of clusters of rigid molecules using the artificial bee colony algorithm. *Phys. Chem. Chem. Phys.* **2016**, *18*, 3003–3010.

26 Vanommeslaeghe, K.; Hatcher, E.; Acharya, C.; Kundu, S.; Zhong, S.; Shim, J.; Darian, E.; Guvench, O.; Lopes, P.; Vorobyov, I., et al. CHARMM general force field: A force field for drug-like molecules compatible with the CHARMM all-atom additive biological force fields. *J. Comput. Chem.* **2010**, *31*, 671–690.

27 Malloum, A.; Fifen, J. J.; Conradie, J. Structures and spectroscopy of the ammonia eicosamer, $(NH_3)_{n=20}$. *J. Chem. Phys.* **2018**, *149*, 024304.

28 Malloum, A.; Fifen, J. J.; Conradie, J. Exploration of the potential energy surface of the ethanol hexamer. *J. Chem. Phys.* **2019**, *150*, 124308.

29 Malloum, A.; Fifen, J. J.; Conradie, J. Large-Sized Ammonia Clusters and Solvation Energies of the Proton in Ammonia. *J. Comput. Chem.* **2020**, *41*, 21–30.

30 Malloum, A.; Fifen, J. J.; Conradie, J. Theoretical infrared spectrum of the ethanol hexamer. *Int. J. Quantum Chem.* **2020**, *120*, e26234.

31 Malloum, A.; Conradie, J. Global and local minima of protonated acetonitrile clusters. *New J. Chem.* **2020**, *44*, 17558–17569.

32 Malloum, A.; Fifen, J. J.; Dhaouadi, Z.; Engo, S. G. N.; Conradie, J. Structures, Relative Stabilities and Binding Energies of Neutral Water Clusters,$(H_2O)_{2-30}$. *New J. Chem.* **2019**, *43*, 13020–13037.

33 Malloum, A.; Conradie, J. Structures of water clusters in the solvent phase and relative stability compared to gas phase. *Polyhedron* **2021**, *193*, 114856.

34 Tawa, G.; Topol, I.; Burt, S.; Caldwell, R.; Rashin, A. Calculation of the aqueous solvation free energy of the proton. *J. Chem. Phys.* **1998**, *109*, 4852–4863.

35 Hunenberger, P.; Reif, M. *Single-Ion Solvation*; Theoretical and Computational Chemistry Series; The Royal Society of Chemistry, 2011; pp 001–664.

36 Fifen, J. J.; Nsangou, M.; Dhaouadi, Z.; Motapon, O.; Jaidane, N.-E. Solvation Energies of the Proton in Methanol. *J. Chem. Theory Comput.* **2013**, *9*, 1173–1181.

37 Pliego Jr, J. R.; Miguel, E. L. Absolute single-ion solvation free energy scale in methanol determined by the lithium cluster-continuum approach. *J. Phys. Chem. B* **2013**, *117*, 5129–5135.

38 Carvalho, N. F.; Pliego, J. R. Cluster-continuum quasichemical theory calculation of the lithium ion solvation in water, acetonitrile and dimethyl sulfoxide: an absolute single-ion solvation free energy scale. *Phys. Chem. Chem. Phys.* **2015**, *17*, 26745–26755.

39 Ishikawa, A.; Nakai, H. Quantum chemical approach for condensed-phase thermochemistry (III): Accurate evaluation of proton hydration energy and standard hydrogen electrode potential. *Chem. Phys. Lett.* **2016**, *650*, 159–164.

40 Malloum, A.; Fifen, J. J.; Dhaouadi, Z.; Nana, E. S. G.; Jaidane, N.-D. Solvation energies of the proton in ammonia explicitly versus temperature. *J. Chem. Phys.* **2017**, *146*, 134308.

41 Malloum, A.; Fifen, J. J.; Conradie, J. Solvation energies of the proton in methanol revisited and temperature effects. *Phys. Chem. Chem. Phys.* **2018**, *20*, 29184–29206.

42 Malloum, A.; Fifen, J. J.; Conradie, J. Determination of the absolute solvation free energy and enthalpy of the proton in solutions. *J. Mol. Liq.* **2021**, *322*, 114919.

43 Malloum, A.; Conradie, J. Solvation free energy of the proton in acetonitrile. *J. Mol. Liq.* **2021**, *335*, 116032.

44 Fifen, J. J.; Nsangou, M.; Dhaouadi, Z.; Motapon, O.; Jaidane, N.-E. Structures of Protonated Methanol Clusters and Temperature Effects. *J. Chem. Phys.* **2013**, *138*, 184301.

45 Frisch, M. J. et al. Gaussian˜16 Revision A.03. 2016; Gaussian Inc. Wallingford CT.

46 Tomasi, J.; Mennucci, B.; Cammi, R. Quantum mechanical continuum solvation models. *Chem. Rev.* **2005**, *105*, 2999–3094.

47 Grimme, S. Improved second-order Møller–Plesset perturbation theory by separate scaling of parallel-and antiparallel-spin pair correlation energies. *J. Chem. Phys.* **2003**, *118*, 9095–9102.

48 Neese, F. The ORCA program system. *Wiley Interdiscip. Rev. Comput. Mol. Sci.* **2012**, *2*, 73–78.

49 Marenich, A. V.; Cramer, C. J.; Truhlar, D. G. Universal solvation model based on solute electron density and on a continuum model of the solvent defined by the bulk dielectric constant and atomic surface tensions. *J. Phys. Chem. B* **2009**, *113*, 6378–6396.

50 Keith, T. A. TK Gristmill software. *Overland Park KS, USA* **2019**, *11*, 16, (aim.tkgristmill.com).

51 Shields, R. M.; Temelso, B.; Archer, K. A.; Morrell, T. E.; Shields, G. C. Accurate predictions of water cluster formation,$(H_2O)_{n=2-10}$. *J. Phys. Chem. A* **2010**, *114*, 11725–11737.

52 Temelso, B.; Archer, K. A.; Shields, G. C. Benchmark Structures and Binding Energies of Small Water Clusters with Anharmonicity Corrections. *J. Phys. Chem. A* **2011**, *115*, 12034–12046.

53 Malloum, A.; Conradie, J. Structures, binding energies and non-covalent interactions of furan clusters. *J. Mol. Graph. Mod.* **2022**, *111*, 108102.

54 Malloum, A.; Conradie, J. Non-Covalent Interactions in Dimethylsulfoxide (DMSO) Clusters and DFT Benchmarking. *J. Mol. Liq.* **2022**, *350*, 118522.

55 Malloum, A.; Conradie, J. Dimethylformamide clusters: non-covalent bondings, structures and temperature-dependence. *Mol. Phys.* **2022**, *xxxx*, 2118188.

56 Wang, Y.; Babin, V.; Bowman, J. M.; Paesani, F. The water hexamer: cage, prism, or both. Full dimensional quantum simulations say both. *J. Am. Chem. Soc.* **2012**, *134*, 11116–11119.

57 Pérez, C.; Muckle, M. T.; Zaleski, D. P.; Seifert, N. A.; Temelso, B.; Shields, G. C.; Kisiel, Z.; Pate, B. H. Structures of cage, prism, and book isomers of water hexamer from broadband rotational spectroscopy. *Science* **2012**, *336*, 897–901.

58 Rakshit, A.; Yamaguchi, T.; Asada, T.; Bandyopadhyay, P. Understanding the structure and hydrogen bonding network of (H 2 O) 32 and (H 2 O) 33 : an improved Monte Carlo temperature basin paving (MCTBP) method and quantum theory of atoms in molecules (QTAIM) analysis. *RSC Adv.* **2017**, *7*, 18401–18417.

59 Cabani, S.; Gianni, P.; Mollica, V.; Lepori, L. Group contributions to the thermodynamic properties of non-ionic organic solutes in dilute aqueous solution. *J. Solution Chem.* **1981**, *10*, 563–595.

60 Guedes, R.; Coutinho, K.; Costa Cabral, B.; Canuto, S. Differential hydration of phenol and phenoxy radical and the energetics of the phenol O- H bond in solution. *J. Phys. Chem. B* **2003**, *107*, 4304–4310.

61 Malloum, A.; Conradie, J. Molecular simulations of the adsorption of aniline from waste-water. *J. Mol. Graph. Mod.* **2022**, *117*, 108287.